Energy level scheme of an InAs/InGaAs/GaAs quantum dots-in-a-well infraredphotodetector structure

Linda Höglund, K. Fredrik Karlsson, Per-Olof Holtz, H. Pettersson, L.E. Pistol, Q. Wang, S. Almqvist, C. Asplund, H. Malm, E. Petrini and J. Y. Andersson

Original Publication:

Linda Höglund, K. Fredrik Karlsson, Per-Olof Holtz, H. Pettersson, L.E. Pistol, Q. Wang, S. Almqvist, C. Asplund, H. Malm, E. Petrini and J. Y. Andersson, Energy level scheme of an InAs/InGaAs/GaAs quantum dots-in-a-well infraredphotodetector structure, 2010, Physical Review B. Condensed Matter and Materials Physics, (82), 3, 035314.
http://dx.doi.org/10.1103/PhysRevB.82.035314

Energy level scheme of InAs/$In_xGa_{1-x}As$/GaAs quantum-dots-in-a-well infrared photodetector structures

L. Höglund,[1] K. F. Karlsson,[2] P. O. Holtz,[2] H. Pettersson,[3,4] M. E. Pistol,[4] Q. Wang,[1] S. Almqvist,[1] C. Asplund,[5] H. Malm,[5] E. Petrini,[1] and J. Y. Andersson[1]

[1]*Acreo AB, Electrum 236, S-16440 Kista, Sweden*

[2]*Department of Physics, Chemistry and Biology (IFM), Linköping University, S-58183 Linköping, Sweden*

[3]*Center for Applied Mathematics and Physics, Halmstad University, P.O. Box 823, S-30118 Halmstad, Sweden*

[4]*Solid State Physics and the Nanometer Structure Consortium, Lund University, P.O. Box 118, S-22100 Lund, Sweden*

[5]*IRnova, Electrum 236, S-16440 Kista, Sweden*

(Received 16 December 2009; published 22 July 2010)

A thorough investigation of quantum-dots-in-a-well structures for infrared photodetector applications has been performed employing different experimental techniques. The electronic structure of self-assembled InAs quantum dots embedded in an $In_{0.15}Ga_{0.85}As$/GaAs quantum well (QW) was deduced from photoluminescence (PL) and PL excitation (PLE) spectroscopy. From polarization-dependent PL it was revealed that the quantum dots hold two electron energy levels and two heavy-hole levels. Tunnel capacitance spectroscopy confirmed an electron energy level separation of about 50 meV, and additionally, that the conduction-band ground state and excited state of the dots are twofold and fourfold degenerates, respectively. Intersubband photocurrent spectroscopy, combined with simultaneous interband pumping of the dots, revealed a dominant transition at 150 meV (8.5 μm) between the ground state of the quantum dots and the excited state of the QW. Results from detailed full three-dimensional calculations of the electronic structure, including effects of composition intermixing and interdot interactions, confirm the experimentally unravelled energy level scheme of the dots and well.

DOI: 10.1103/PhysRevB.82.035314 PACS number(s): 73.21.La

I. INTRODUCTION

Quantum-dots-in-a-well infrared photodetectors (DWELL IPs) are presently being considered as candidates for the next generation of infrared photodetectors, primarily due to an expected reduced dark current, which enables higher operating temperatures[1,2] but also because of the tunability of the detection wavelength and the possibility of dual color detection within each pixel.[3–5] Several groups have studied the DWELL IP experimentally,[6–10] as well as theoretically,[11–13] showing possible detection in several different wavelength regions; from the medium wavelength infrared (3–5 μm) region and the long-wavelength infrared (8–14 μm) region to detection in the far-infrared region (>20 μm), utilizing different intersubband transitions emanating from the quantum dot (QD) ground state. However, the interpretations of which final states are involved in the intersubband transitions causing the main photocurrent peak, and the actual cause of the tunability of the detection wavelength, diverge. Experimentally it has been shown that the detection wavelength can be tuned from 7 to 11 μm by changing the width of the quantum well (QW) while the theoretically predicted shift of the QW ground state is smaller.[7,11,12] This indicates that it is not necessarily the QW ground state, which is the final state of the intersubband transition involved in the photocurrent. Furthermore, the experimentally observed energy level schemes differ significantly from the theoretically predicted ones.[11,14] Uncertainty concerning the exact energy level structure hinders the full optimization and evaluation of the DWELL IP.

In this paper, the energy level scheme of an InAs/$In_{0.15}Ga_{0.85}As$/GaAs DWELL IP is investigated by means of several interband and intersubband measurement techniques. Interband transitions are revealed using photoluminescence (PL) and PL excitation (PLE) spectroscopy from which an approximate energy level scheme is deduced. A distinction between transitions involving heavy hole (HH) and light hole (LH) is made by investigation of the polarization dependence of the ground-state and excited-state interband transitions. Complementary intersubband measurement techniques are used to determine the energy level spacing in the conduction band of the dots and the well. The level spacing between the ground and excited states of the dots is confirmed using tunnel capacitance measurements. Photocurrent spectroscopy is employed to confirm the level spacing between the ground state of the dots and the excited state of the well and continuum, respectively. We have also combined photocurrent spectroscopy with selective interband excitation to study the effect of state filling on the photo response of the DWELL IP. The state filling experiments offer an interesting way of simulating the effects of varying the doping level. Moreover, we have also done a full three-dimensional simulation of the electronic structure of the DWELL IPs and found a good agreement with the experimental results.

II. MATERIAL GROWTH AND DEVICE DESIGN

The DWELL structure used in this study consists of a 500 nm *n*-doped ($\sim 1\times 10^{17}$ cm^{-3}) lower GaAs (001) contact layer, a stacked QD active region and finally the structure is terminated with a 300 nm *n*-doped ($\sim 1\times 10^{17}$ cm^{-3}) upper GaAs contact layer. The active region in the DWELL structure is a ten-layer stack, where each period consists of an undoped InAs QD layer embedded in an 8 nm $In_{0.15}Ga_{0.85}As$

QW and a 33 nm GaAs barrier. The QD layer is inserted asymmetrically in the 8 nm wide QW, with 2 nm $In_{0.15}Ga_{0.85}As$ under and 6 nm $In_{0.15}Ga_{0.85}As$ above the QD layer. The structures were grown by metal-organic vapor phase epitaxy in a vertical Veeco reactor operating at 100 mbar using triethylgallium, trimethylindium, and arsine as source materials. First, a 300 nm GaAs buffer layer and the lower contact layer were grown at 710 °C. Thereafter the temperature was lowered to 485 °C before the growth of the $In_{0.15}Ga_{0.85}As$ QW and the QD layer. The lower $In_{0.15}Ga_{0.85}As$ QW was grown immediately before the QDs at a growth rate of 0.67 nm/s. The InAs layer was grown at a V/III ratio of 13, with a nominal thickness of 1.8 ML and a growth rate of 0.14 nm/s following earlier optimization procedures for a high density and uniformity of QDs.[15] The QDs ripened during a subsequent growth interruption of 30 s with all precursors switched off. The upper $In_{0.15}Ga_{0.85}As$ QW was grown at a growth rate of 0.18 nm/s. Before raising the temperature to 600 °C, a 3 nm GaAs cap layer was grown at 485 °C to avoid desorption of the InGaAs layer. The structure was annealed for 5 min at 600 °C before capping with 30 nm GaAs at a growth rate of 0.15 nm/s. The upper contact layer was grown at 600 °C. Similar structures were grown for size and density characterization with atomic force microscopy (AFM). In the sample used for AFM measurements, an uncapped QD layer was terminating the structure. The measurement revealed a high dot density of approximately 9.3×10^{10} cm^{-2} and an average QD width and height of 16 nm and 3.5 nm, respectively. Complementary measurements on the composition of QDs embedded in the InGaAs/GaAs QWs were performed with cross-sectional scanning tunneling microscopy (X-STM), revealing a uniform distribution of Ga in the QDs (33%) due to intermixing.[16] The average width and height of the embedded QDs as studied by X-STM were 14 nm and 4.5 nm, respectively, i.e., slightly different from the surface QDs. This is expected since some redistribution of material might occur during the cooldown procedure for the uncapped surface QDs.

For the photocurrent measurements, vertical DWELL IP structures were fabricated by standard optical lithography, etching, and metallization techniques. The resulting single pixel components had dimensions of 170 $\mu m\times170$ μm and 360 $\mu m\times360$ μm, respectively, with alloyed AuGe/Ni/Au ohmic contacts.

For the capacitance measurements, a special sample was grown containing one buried GaAs contact layer with a doping level of 2×10^{18} cm^{-3}, a 25 nm GaAs tunneling barrier, a single layer of InAs QDs embedded in a 8 nm wide $In_{0.15}Ga_{0.85}As$ QW using the same growth conditions as described above, and finally a 110 nm GaAs cap layer. Two rows of AuGe/Ni contacts were fabricated on the surface of the structure. The first row was annealed, enabling formation of ohmic contacts to the buried contact layer while the second contact row was not annealed, resulting in a Schottky contact. The size of each contact pad is 330 $\mu m\times330$ μm.

III. EXPERIMENTAL DETAILS

PL and PLE measurements were performed at 2 K using an argon laser pumped Ti:sapphire (Ti:Sp) laser, tunable between 700 and 1020 nm, as excitation source. The polarization dependence of the interband transitions was studied by means of a diffraction limited micro-PL setup. The linearly polarized light from the laser was rotated by a half-lambda plate, enabling linear polarization of the laser beam in the vertical or the lateral direction of the QD, respectively. The laser was focused through a thin optical window of a continuous flow cryostat to a spot size of 2 μm in diameter on a cleaved edge of the sample with a microscope objective. The luminescence was collected with the same objective lens. A long-wavelength filter, suppressing all wavelengths shorter than 980 nm was used in front of the monochromator and the luminescence was detected by a liquid nitrogen cooled InGaAs array detector.

The intersubband photocurrent measurements were performed with a Bomem DA8 Fourier transform spectrometer, using a globar light source and a KBr beamsplitter, in combination with a Keithley 427 current amplifier. The sample was excited by unpolarized light at 45° incidence. In the photocurrent measurements, a positive bias was applied to the bottom contact of the DWELL IP. Two different laser sources were used to increase the electron population in the QDs during the photocurrent measurements with optical pumping: a laser diode pumped solid-state laser with an emission wavelength of 1064 nm (1165 meV) and a Ti:Sp laser with emission at 1010 nm (1227 meV). The capacitance measurements were recorded using an Agilent E4980A LCR meter.

IV. THEORETICAL DETAILS

The energy level structure of the dots was calculated using a full three-dimensional simulation. First, the strain tensor elements were computed using linear elasticity theory.[17] The numerical problem was solved on a $160\times160\times160$ grid, giving a physical box size of 130 nm $\times$ 130 nm $\times$ 130 nm, using open boundary conditions. The use of open boundary conditions is necessary since the periodic boundary conditions are not well founded if the system is strained. Using the so obtained strain tensor elements as input to an eight-band $\mathbf{k}\cdot\mathbf{p}$ model[18] the local band edges were determined and the remaining parameters were obtained from Ref. 19. The confined electron energy levels were then found by a one-band envelope function approximation in which the strain modified effective mass was used. Supported by the X-STM measurements, a uniform alloy of $Ga_{0.33}In_{0.67}As$ was assumed for the QDs. The QDs were furthermore assumed to have the shape of a half ellipsoid with the dimensions deduced from the X-STM measurements. Due to the very high dot density, interdot interactions were taken into account by including five laterally coupled dots separated by 35 nm. The QD centers were positioned at (0, 0), (35, 0), (−35, 0), (0, 35), and (0, −35) in the (x,y) plane.

V. RESULTS AND DISCUSSION

The lowest interband transition energy of the DWELL structure is investigated by a combination of interband measurement techniques, i.e., PL and photocurrent measurements

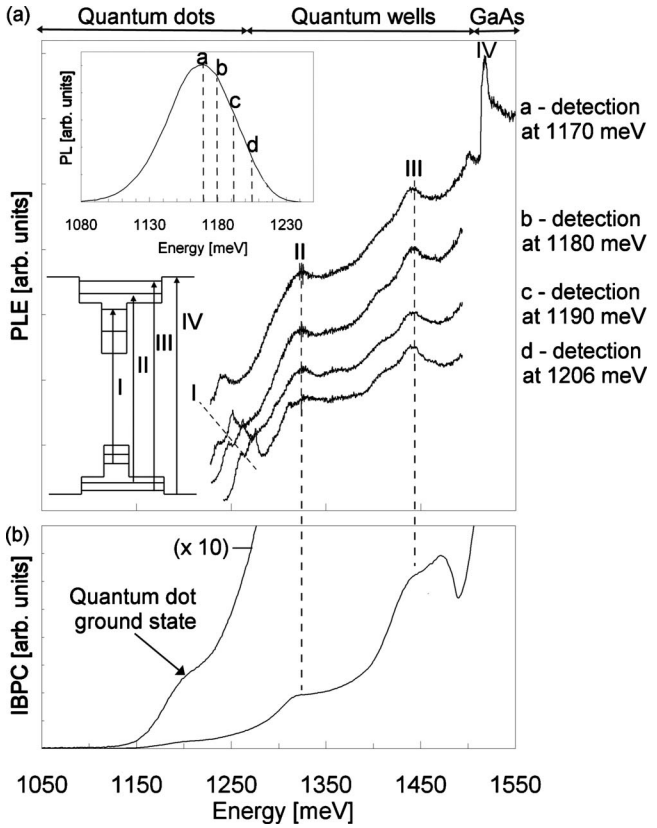

FIG. 1. (a) PLE measurements of the DWELL structure for four different detection energy intervals. The center of each detection interval is marked with dashed lines accompanied by one of the letters (a)–(d) in the PL spectrum (upper inset). The lower inset shows which interband transitions are responsible for the observed PLE peaks. (b) Interband photocurrent spectrum at an applied bias of 3 V and temperature of 77 K.

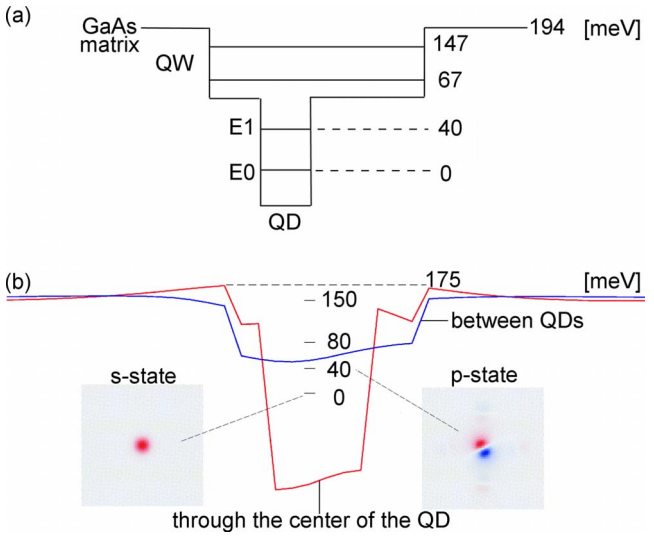

FIG. 2. (Color online) (a) Experimentally obtained conduction-band energy level scheme of the DWELL structure investigated, deduced from the interband measurements shown in Fig. 1. (b) The theoretically predicted conduction-band energy level scheme of the DWELL structure. The conduction-band minimum in the structure through the center of the dot is illustrated by a red trace. The blue trace is the conduction-band minimum between the dots. The short black traces are the energy levels of the structure. The insets display the ground-state wave function and the first excited-state wave function, respectively.

(Fig. 1). The high QD density enables tunneling between the QDs and electrons and holes will redistribute to the lowest energy levels before recombination. This will cause a Stokes shift of the PL emission peak compared to the absorption peak recorded in the photocurrent measurements. In order to reveal the magnitude of this Stokes shift, a comparison between the interband photocurrent peak and the PL peak is performed. In the photocurrent measurement a broad shoulder corresponding to the QD ground-state transitions appears at 1200 meV [Fig. 1(b)] while the PL emission peaks at 1170 meV. The emission is consequently Stokes shifted by approximately 30 meV compared to the photocurrent peak.

Energy levels higher than the QD ground states are typically not filled at moderate excitation power in the PL measurements. Instead, excited states in the QDs, as well as in the QWs, were revealed by PLE measurements. Four different detection intervals corresponding to different QD ensembles were chosen. Peak I shifts with the detection energy (with a constant energy separation of 58 meV) while peaks II and III remain at the same energy position in the PLE measurements [Fig. 1(a)]. Based on these facts, one can conclude that peak I is related to the energy levels in the QDs while peaks II and III are related to the energy levels in the QW. Peak IV corresponds to the GaAs band-edge transition at 1519 meV. From the results of the selective PL (SPL) measurements below, it will be shown that the PLE peaks related to QD interband transitions are in fact not Stokes shifted. Therefore, the energy separation of 58 meV, deduced from PLE measurements is the true separation between the excitonic ground states of the QDs and their excited states. The peaks observed in the interband measurements are all excitonic peaks and exciton binding energies in InAs QDs and InGaAs QWs of 30 meV and 10 meV, respectively,[20–22] must therefore be taken into account to accurately deduce an energy level scheme from PL, PLE, and photocurrent measurements.

The conduction-band energy level separations are estimated as 67% (Ref. 23) of the energy difference between the GaAs band edge and the energy values of the PL and PLE peaks of the QD and QW interband transitions, compensated for the Stokes shift and the excitonic effects. The resulting conduction-band energy level scheme is shown in Fig. 2(a).

From theoretical calculations of the single-particle conduction-band energy levels of the DWELL structure, four electron energy levels were obtained [Fig. 2(b)]. The lowest two levels are confined in the dot, where the envelope function of the lowest level is *s* like and the second level is *p* like [see insets in Fig. 2(b)]. The third and fourth levels are delocalized in the QW but the shape of the wave function is strongly affected by the dot. The fourth level is very close to the conduction-band edge of the GaAs barrier and an adjustment of the valence-band offset by 0.02 eV was necessary in order to get a second confined state in the well, as observed in the experiments. The strain field from the QDs strongly modifies the conduction band of the surrounding QW as well

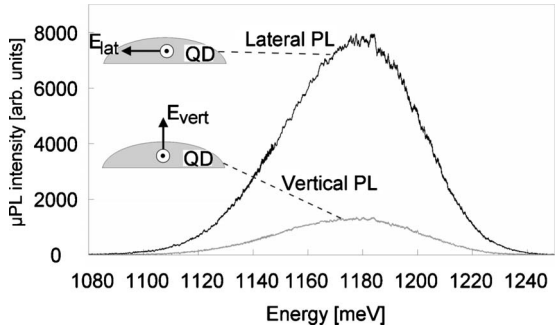

FIG. 3. Photoluminescence from a DWELL structure excited with an unpolarized source (wavelength—720 nm), detecting the luminescence with two different linear polarizations; parallel to the plane of the QD (marked lateral PL) and perpendicular to the plane of the QD (marked vertical PL), respectively. The insets show the orientation of the *E* field of the measured luminescence with respect to the QD.

as the GaAs barrier. In fact, the conduction-band energy of the QW is shifted by about 100 meV toward higher energy due to the strain effects from the dot. Also the QW potential between the dots is affected by the strain effects from the QDs induced by the short peak-to-peak distance between the QDs (on average 35 nm). When taking these effects into account a reasonable correlation was obtained between the experimentally determined [Fig. 2(a)] and the theoretically calculated [Fig. 2(b)] energy level schemes.

In order to achieve additional information about the QD hole states involved, the polarization dependence of the interband transitions were studied. According to the interband selection rules of quantum structures,[24] the strongest coupling to light holes occurs when the polarization vector is oriented vertically, i.e., perpendicular to the base plane of the QD (see Fig. 3). Coupling to heavy holes occurs for a polarization vector oriented laterally, i.e., parallel to the base plane. From the polarization dependence of the ground-state luminescence (Fig. 3), it is readily observed that the intensity of the laterally polarized luminescence is approximately six times larger than the vertically polarized luminescence. This indicates that the hole ground state mainly exhibit HH character [HH0 in the inset in Fig. 4]. This is expected since LH states are shifted toward higher energy by the inherent strain in the QDs.[2]

Correspondingly, the character of the holes involved in the interband transitions associated with excited states of the QDs (peak I in Fig. 1) was investigated using SPL. Here, excited states of different QD ensembles were excited resonantly with narrow bandwidth, linearly polarized infrared light (inset, Fig. 4). Broad luminescence spectra are observed and in addition, resonant luminescence peaks (marked with dotted arrows in Fig. 4) appear shifted from the selected excitation energies (marked with solid arrows in Fig. 4) by 58 meV, which is consistent with the interband energy separation deduced from the PLE experiments. These resonant luminescence peaks actually constitutes the detection in the PLE measurements since they deviate from the broad luminescence spectra, which are similar for all excitation energies on the high energy side [Figs. 4(b)–4(d)]. The presence of

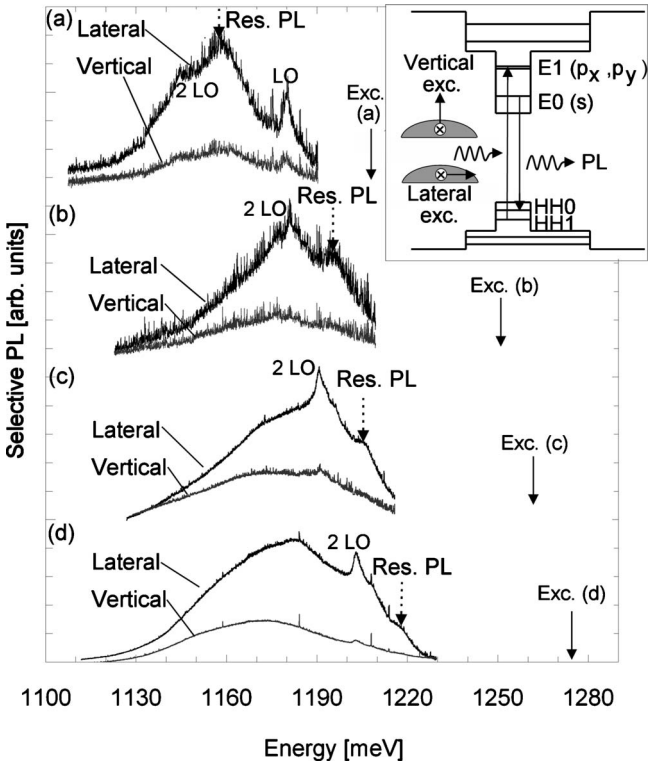

FIG. 4. Selective PL using a linearly polarized excitation source with the polarization direction parallel to the lateral or vertical direction of the QDs (the insets indicate the direction of the *E* field with respect to the QD). The excitation energies at (a) 1215 meV, (b) 1252 meV, (c) 1262 meV, and (d) 1274 meV induce resonant luminescence peaks (marked with arrows) separated from the respective excitation energy by 58 meV. The sharp lines correspond to phonon resonances, with energy separations of 36 meV (one GaAs LO phonon) and 72 meV (two GaAs LO phonons) from the excitation energies. The inset shows the interpretation of the hole states (HH0, HH1) and the electron states (E0, E1) involved in the interband transitions, deduced from the measurement results in (a)–(d).

the broad luminescence peak is attributed to tunneling of photoexcited carriers between the densely packed QDs. Only when the excitation energy is resonant with QDs with low excited-state energies [Fig. 4(a)], does the resonant PL peak dominate the luminescence spectrum since the possibility of interdot tunneling decreases.

A dominant luminescence is observed when the excitation light is laterally polarized. The ratio between the luminescence magnitudes for lateral and vertical polarizations, respectively, varies between 2.7 and 4.2 at the different excitation energies. From the polarized SPL spectra, it is evident that peak I in Fig. 1 is a transition involving heavy-holelike states. Considering that the interband transitions between quantized energy levels with the same quantum number (n) are the most probable, peak I is assigned to a transition from the first excited heavy-hole level (HH1 in the inset, Fig. 4) to the first excited electron level (E1 in the inset, Fig. 4).

Further investigations of the electron levels of the QDs were made using tunneling capacitance spectroscopy.[25–27] From measurements of the capacitance between the top Schottky contact and the buried contact layer, two broad

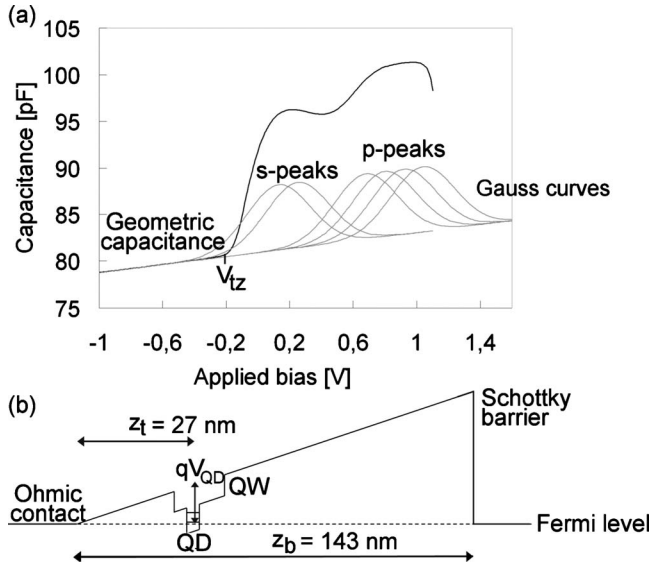

FIG. 5. (a) Tunneling capacitance versus bias for a sample structure depicted in (b) at T=4.2 K and a frequency and amplitude of the ac bias of 10 kHz and 10 mV, respectively. At biases <-0.2 V the Fermi level is situated below the energy levels of the QDs and the measured capacitance reflects the geometric capacitance of the Schottky contact. Loading of electrons into the ground state of the dots starts at the threshold voltage $V_{tz}=-0.2$ V. The C-V curve in (a) is deconvoluted into Gaussian curves related to filling of the twofold degenerate s, p_x, and p_y states in the QDs.

resonances were observed at 0.2 V and 0.83 V, respectively (Fig. 5). The resonances correspond to tunneling from the buried contact layer through the 25 nm undoped GaAs layer into the discrete conduction-band energy states of the QDs. The integrated area under each resonance (compensated by the lever arm, z_b/z_t=143/27) [Fig. 5(b)] (Ref. 26) corresponds to the amount of charge, which has tunneled into the QDs located under the Schottky contact. Since the density of QDs is known from the AFM measurements, the average number of electrons filling each QD can be calculated. From the area (compensated by the lever arm) between the CV curve and a reference line corresponding to the geometric capacitance of the Schottky contact, it was found that in total six electrons can occupy each QD. The first resonance at 0.2 V corresponds to loading of two electrons into the ground level E0 of the dots. The resonance centered at about 0.83 V is due to filling of the excited E1 level with four electrons. In our model, the ground state is s-like with a twofold degeneracy, whereas the p-like excited states (p_x and p_y) have a degeneracy of four. The observed capacitance traces are relatively broad which prevents the observation of single electrons tunneling into the s and p states. The broadening stems from the size distribution of the dots (inhomogeneous broadening). Nevertheless, from the bias separation between the two broad resonances, the single-particle energy separation between E0 and E1 can be estimated by considering the geometrical position of the QD layer and the additional charging energy (caused by the Coulomb interaction between the electrons) required to load electrons into the QDs. The charging energy, E_C, approximately varies with the number of injected electrons (N) as

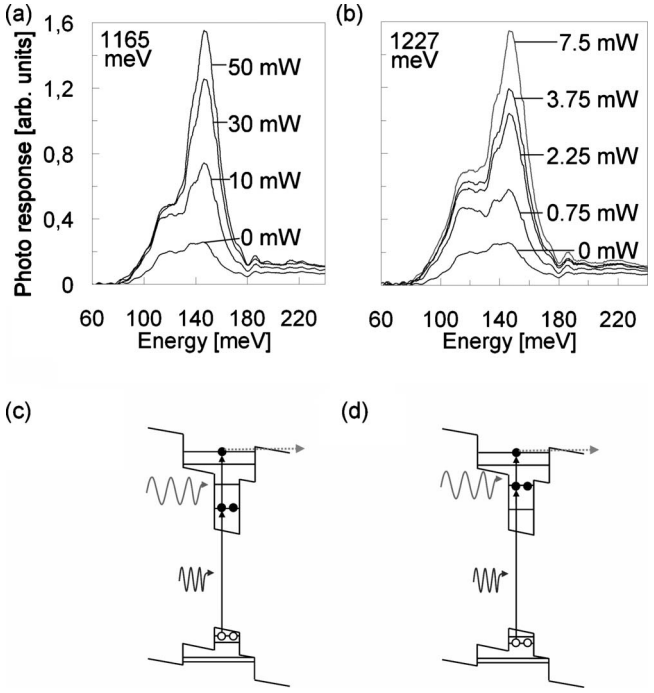

FIG. 6. Photocurrent spectra obtained at an applied bias of 2.25 V with simultaneous optical pumping of [(a) and (c)] the ground levels and [(b) and (d)] the excited levels of the QDs. The temperature during the measurements was 60 K.

$$E_C(N) = \left(N - \frac{1}{2}\right) \cdot \frac{q^2}{C_{\mathrm{QD}}},$$

where q is the electronic charge and C_{QD} is the self-capacitance of the QD.[27,28] C_{QD} is approximated by the capacitance of a disk with diameter d, given by $C_{\mathrm{QD}}=4\varepsilon\varepsilon_0 d$, where ε is the relative static dielectric constant of the surrounding GaAs matrix.[27] The resulting Coulomb charging energy between the two electrons in the ground state of an average sized dot with a diameter of 14 nm is approximately 26 meV. The difference in applied bias ΔV for the two broad resonances observed in Fig. 5(a) (with peak values at 0.2 V and 0.83 V, respectively) transforms into a difference in Fermi-level position ΔE at the spatial location of the dots according to $\Delta E = q\Delta V / \frac{z_b}{z_t}$ [Fig. 5(b)]. Taking the estimate of the charging energy discussed above into account, we deduce a separation between the ground state, E_0 and the excited state, E_1, of about 50 meV in reasonable agreement with the intersubband energy separation obtained from the optical data [Fig. 2(a)]. The discrepancy is attributed to the uncertainty in the values of the charging energies involved and to the inhomogenous broadening which prevents a more accurate determination of the peak positions of the different states.

Photocurrent measurements were performed on the DWELL samples in order to investigate the energy separations between the QD and QW energy levels. Two different photocurrent peaks at 120 and 148 meV clearly dominate the spectra [Figs. 6(a) and 6(b)]. The initial states involved in these intersubband transitions are identified by using optical

pumping to selectively fill different energy levels of the QDs [Figs. 6(c) and 6(d)]. When increasing the electron population in the QD ground states (E0) by resonant interband pumping, there is a major increase of 148 meV peak [Fig. 6(a)]. Increasing the electron population in the excited states (E1) of the QDs by selective excitation has a strong influence also on the peak at 120 meV [Fig. 6(b)]. We thus attribute the initial states of 148 and 120 meV photocurrent peaks to E0 and E1, respectively. The final states of the intersubband transitions involved in the photocurrent peaks are identified by comparing the energies of the photocurrent peaks with the energy separations revealed from the interband measurements [Fig. 2(a)]. The energy separation between the ground state (E0) of the QDs and the ground state of the QW is too small to match the measured photocurrent peaks at 120 meV and 148 meV, respectively. Furthermore, the ground state of the QW is situated approximately 127 meV below the GaAs conduction-band edge, which is energetically too deep to provide an efficient escape route from this level and the electron energy separation between E0 and the QW excited level is accordingly closer to the measured photocurrent peak. The energy position of the QW excited level with respect to the GaAs conduction-band edge is still rather deep (~47 meV below the band edge). The strong electric field due to the applied bias, however, effectively decreases the tunnel barrier between the QW and the matrix.[10] Using similar analysis based on the interband data from Fig. 2(a), supported by the energy spacings between E0 and E1 of the QDs deduced from tunneling capacitance spectroscopy, we conclude that the 120 meV peak observed in the photocurrent spectra corresponds to transitions from E1 to the excited state of the QW.

The energy separation between the ground state (E0) of the QDs and the GaAs conduction-band edge deduced from the interband measurements is around 194 meV. At low applied biases, the photocurrent spectra reveal a broad peak with an onset at approximately 190 meV (Fig. 7), which is well correlated with the results from the interband measurements. In addition, when adding electrons (and holes) to the ground states of the QDs through optical pumping, an increase in the magnitude of this broad peak is observed, simultaneously with an increase of 148 meV peak. These observations strongly support the interpretation of the broad photocurrent peak in terms of transitions from the ground state of the QDs to the continuum states in the GaAs matrix. The experimental results discussed above are consistent with the energy level scheme of the DWELL structure shown in Fig. 2(a) with two bound energy levels in the QD and two energy levels in the QW. The discrepancy between the evaluated transition energies and the peaks of the photocurrent

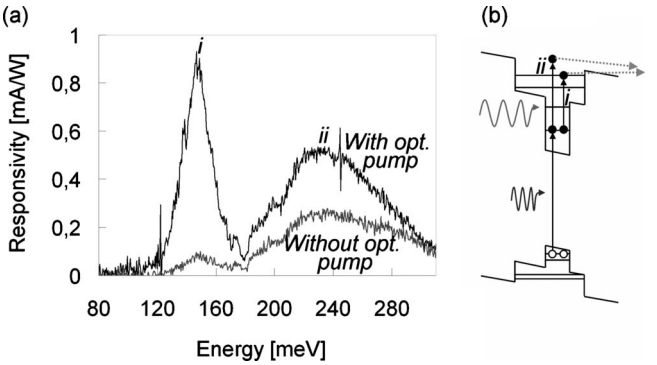

FIG. 7. Photocurrent spectra at an applied bias of 1.5 V with simultaneous optical pumping of the ground levels of the QDs (1165 meV). The temperature during the measurements was 77 K.

spectra can be due to the widths of the optical bands, i.e., the inhomogeneous size distribution of the QDs observed and the uncertainty in the factor used to extract the conduction-band energy separation.

VI. CONCLUSIONS

In summary, we have carried out a comprehensive study of DWELL photodetector structures using a variety of optical interband and intersubband techniques. Polarization sensitive measurements provide additional information on the character of the hole states. Complementary tunnel capacitance measurements support the electronic structure obtained from the optical measurements. A detailed energy level scheme of the conduction band in the DWELL has been obtained from the optical experiments and supported by the tunnel capacitance measurements. The DWELL electronic structure as evaluated from the experimental findings is correlating well with the theoretical predictions. The presented work show the importance of combining different electrical and optical techniques to obtain a consistent model of complicated quantum structures which is crucial for the development of future nanoelectronic devices.

ACKNOWLEDGMENTS

The authors would like to thank the Knowledge Foundation and the Swedish Foundation for Strategic Research for support grants and the Swedish Agency for Innovation Systems and the IMAGIC center of excellence for financial support. The authors would also like to thank Stefan Olsson and Stefan Johansson, FLIR Systems and Mattias Hammar, Royal Institute of Technology (KTH) for many fruitful discussions.

[1] V. Ryzhii, Semicond. Sci. Technol. **11**, 759 (1996).

[2] P. Martyniuk and A. Rogalski, in *Infrared Technology and Applications XXXIV*, edited by B. F. Andresen, G. F. Fulop, and P. R. Norton, Proceedings of SPIE (SPIE Digital Library, 2008), Vol. 6940, p. 694004.

[3] E. Varley, M. Lenz, S. J. Lee, J. S. Brown, D. A. Ramirez, A. Stintz, S. Krishna, A. Reisinger, and M. Sundaram, Appl. Phys. Lett. **91**, 081120 (2007).

[4] P. Aivaliotis, N. Vukmirovic, E. A. Zibik, J. W. Cockburn, D. Indjin, P. Harrison, C. Groves, J. P. R. David, M. Hopkinson, and L. R. Wilson, J. Phys. D **40**, 5537 (2007).
[5] L. Höglund, P. O. Holtz, H. Pettersson, C. Asplund, Q. Wang, S. Almqvist, H. Malm, E. Petrini, and J. Y. Andersson, Appl. Phys. Lett. **93**, 203512 (2008).
[6] E.-T. Kim, Z. Chen, and A. Madhukar, Appl. Phys. Lett. **79**, 3341 (2001).
[7] S. Raghavan, D. Forman, P. Hill, N. R. Weisse-Bernstein, G. von Winckel, P. Rotella, and S. Krishna, J. Appl. Phys. **96**, 1036 (2004).
[8] P. Aivaliotis, S. Menzel, E. A. Zibik, J. W. Cockburn, L. R. Wilson, and M. Hopkinson, Appl. Phys. Lett. **91**, 253502 (2007).
[9] G. Jolley, L. Fu, H. H. Tan, and C. Jagadish, Appl. Phys. Lett. **91**, 173508 (2007).
[10] L. Höglund, P. O. Holtz, H. Pettersson, C. Asplund, Q. Wang, S. Almqvist, S. Smuk, E. Petrini, and J. Y. Andersson, Appl. Phys. Lett. **93**, 103501 (2008).
[11] N. Vukmirović, D. Indjin, Z. Ikonić, and P. Harrison, Appl. Phys. Lett. **88**, 251107 (2006).
[12] X. Han, J. Li, J. Wu, G. Cong, X. Liu, Q. Zhu, and Z. Wang, J. Appl. Phys. **98**, 053703 (2005).
[13] A. Amtout, S. Raghavan, P. Rotella, G. von Winckel, A. Stintz, and S. Krishna, J. Appl. Phys. **96**, 3782 (2004).
[14] S. Krishna, J. Phys. D **38**, 2142 (2005).
[15] L. Höglund, E. Petrini, C. Asplund, H. Malm, J. Y. Andersson, and P. O. Holtz, Appl. Surf. Sci. **252**, 5525 (2006).
[16] L. Ouattara, A. Mikkelsen, E. Lundgren, L. Höglund, C. Asplund, and J. Y. Andersson, J. Appl. Phys. **100**, 044320 (2006).
[17] L. Landau and E. Lifshitz, *Elasticity* (Pergamon, London, 1959).
[18] T. B. Bahder, Phys. Rev. B **41**, 11992 (1990).
[19] I. Vurgaftman, J. R. Meyer, and L. R. Ram-Mohan, J. Appl. Phys. **89**, 5815 (2001).
[20] J. Shumway, A. J. Williamson, A. Zunger, A. Passaseo, M. DeGiorgi, R. Cingolani, M. Catalano, and P. Crozier, Phys. Rev. B **64**, 125302 (2001).
[21] O. Stier, M. Grundmann, and D. Bimberg, Phys. Rev. B **59**, 5688 (1999).
[22] H. Q. Hou, W. Staguhn, S. Takeyama, N. Miura, Y. Segawa, Y. Aoyagi, and S. Namba, Phys. Rev. B **43**, 4152 (1991).
[23] G. Arnaud, J. Allégre, P. Lefebvre, H. Mathieu, L. K. Howard, and D. J. Dunstan, Phys. Rev. B **46**, 15290 (1992).
[24] J. H. Davies, *The Physics of Low-Dimensional Semiconductors* (Cambridge University Press, Cambridge, England, 1998).
[25] H. Pettersson, R. J. Warburton, J. P. Kotthaus, N. Carlsson, W. Seifert, M.-E. Pistol, and L. Samuelson, Phys. Rev. B **60**, R11289 (1999).
[26] R. C. Ashoori, H. L. Stormer, J. S. Weiner, L. N. Pfeiffer, S. J. Pearton, K. W. Baldwin, and K. W. West, Phys. Rev. Lett. **68**, 3088 (1992).
[27] H. Drexler, D. Leonard, W. Hansen, J. P. Kotthaus, and P. M. Petroff, Phys. Rev. Lett. **73**, 2252 (1994).
[28] S. Anand, N. Carlsson, M.-E. Pistol, L. Samuelson, and W. Seifert, J. Appl. Phys. **84**, 3747 (1998).